Electronic Supplementary Material (ESI) for RSC Advances.

Heavier chalcogenone complexes of bismuth(III)trihalides: Potential catalysts for acylative cleavage of cyclic ethers

Katam Srinivas, Paladugu Suresh, Chatla Naga Babu, Arruri Sathyanarayana and Ganesan Prabusankar*

Department of Chemistry, Indian Institute of Technology Hyderabad, ODF Campus, Yeddumailaram, AP, INDIA-502 205. Fax: +91 40 2301 6032; Tel: +91 40 2301 6089; E-mail: prabu@iith.ac.in

Supporting Information

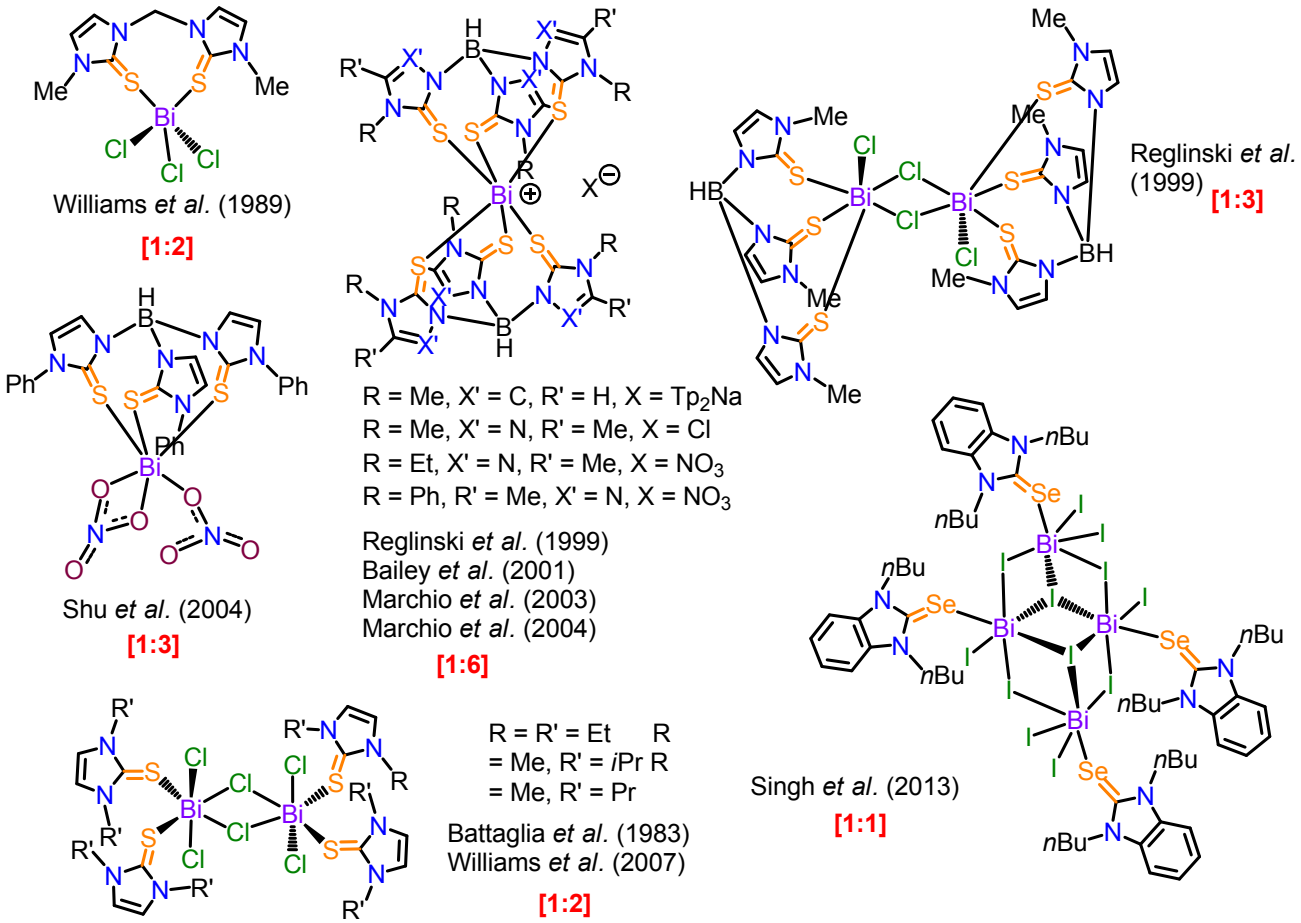

Scheme S1. The structurally characterized monomeric, dimeric and tetrameric bismuth complexes of imazolyl heavier chalcogenone.

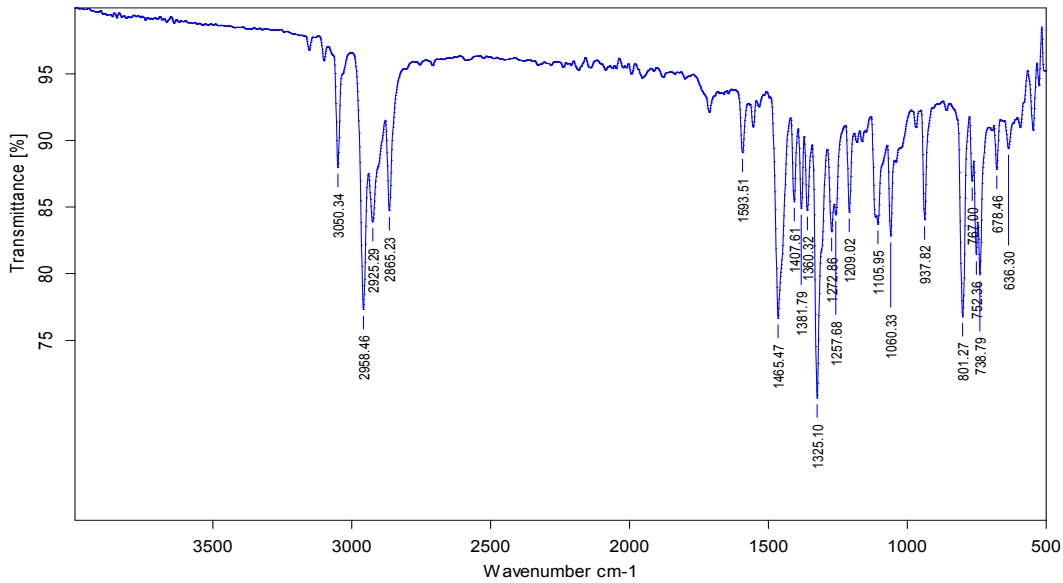

Figure S1. FT-IR (neat) spectrum of IPr=Te (**5**) at RT.

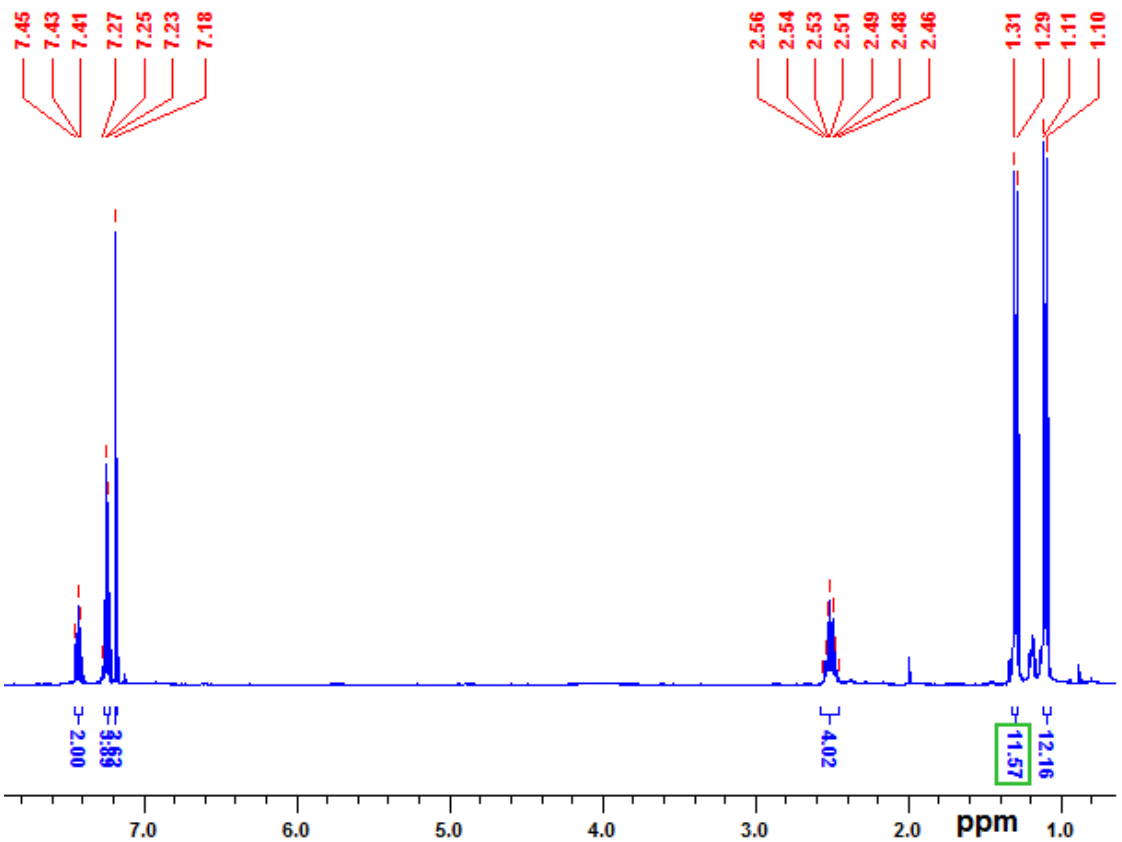

Figure S2. ^{1}H NMR spectrum of IPr=Te (**5**) in $CDCl_3$ at RT.

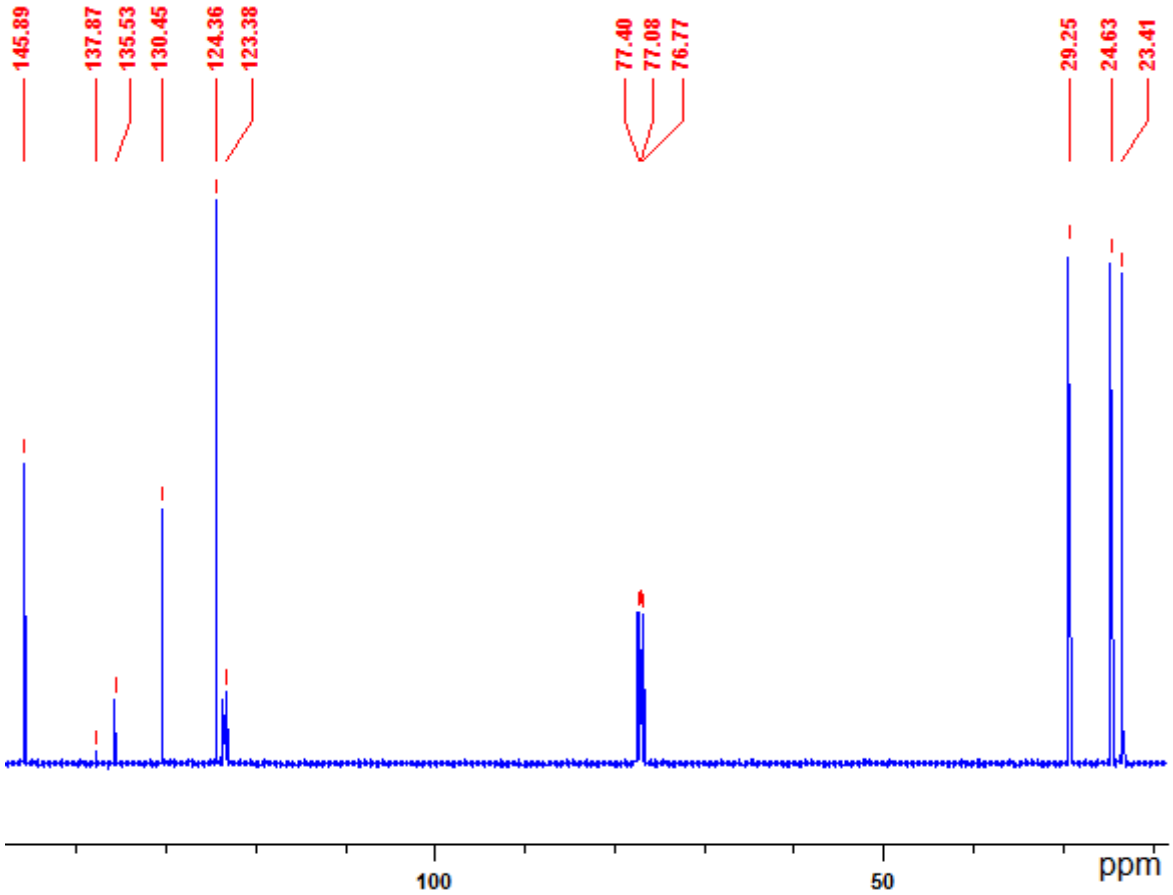

Figure S3. ^{13}C NMR spectrum of IPr=Te (**5**) in $CDCl_3$ at RT.

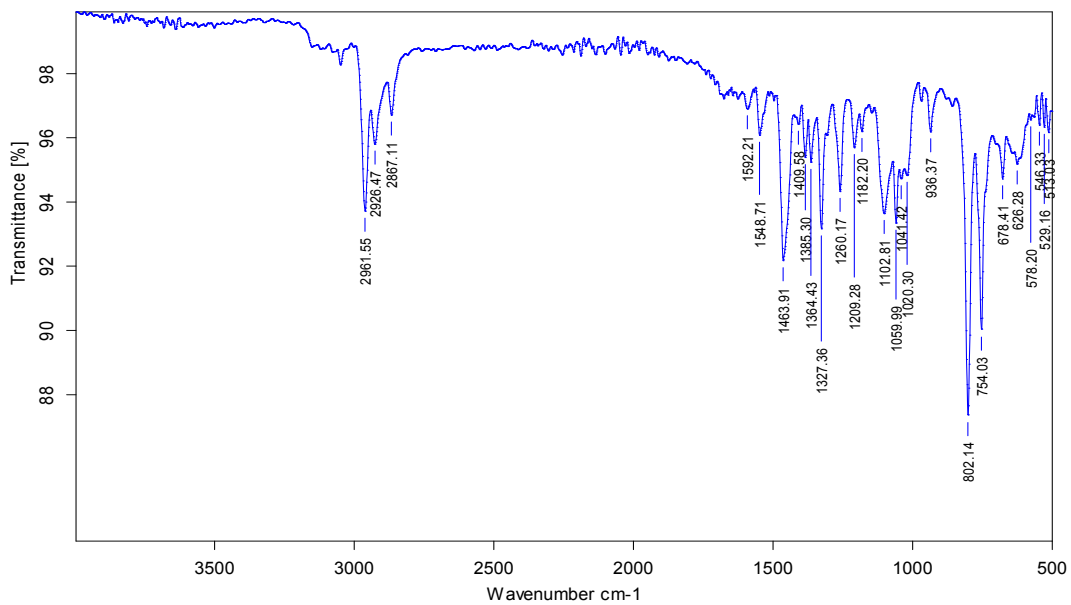

Figure S4. FT-IR (neat) spectrum of [(IPr=Te)$BiCl_3$] (**10**) at RT.

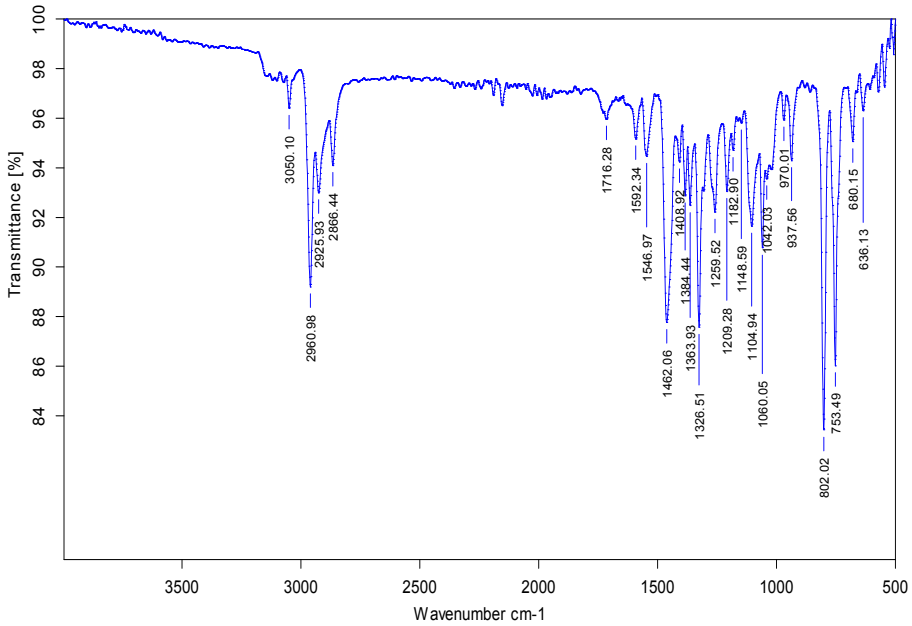

Figure S5. FT-IR (neat) spectrum of [(IPr=Te)$BiBr_3$] (**11**) at RT.

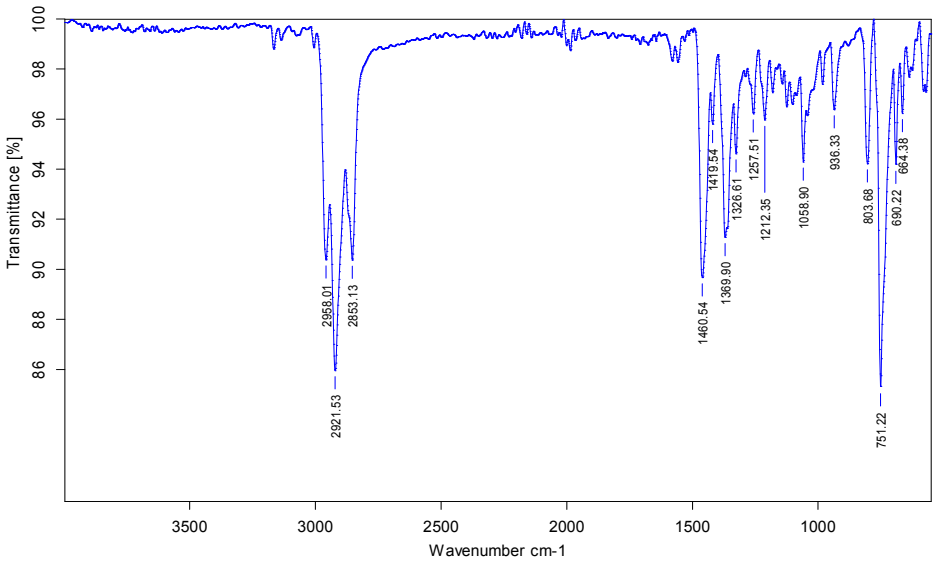

Figure S6. FT-IR (neat) spectrum of [(IPr=S)$BiCl_3$].$CHCl_3$ (**6**) at RT.

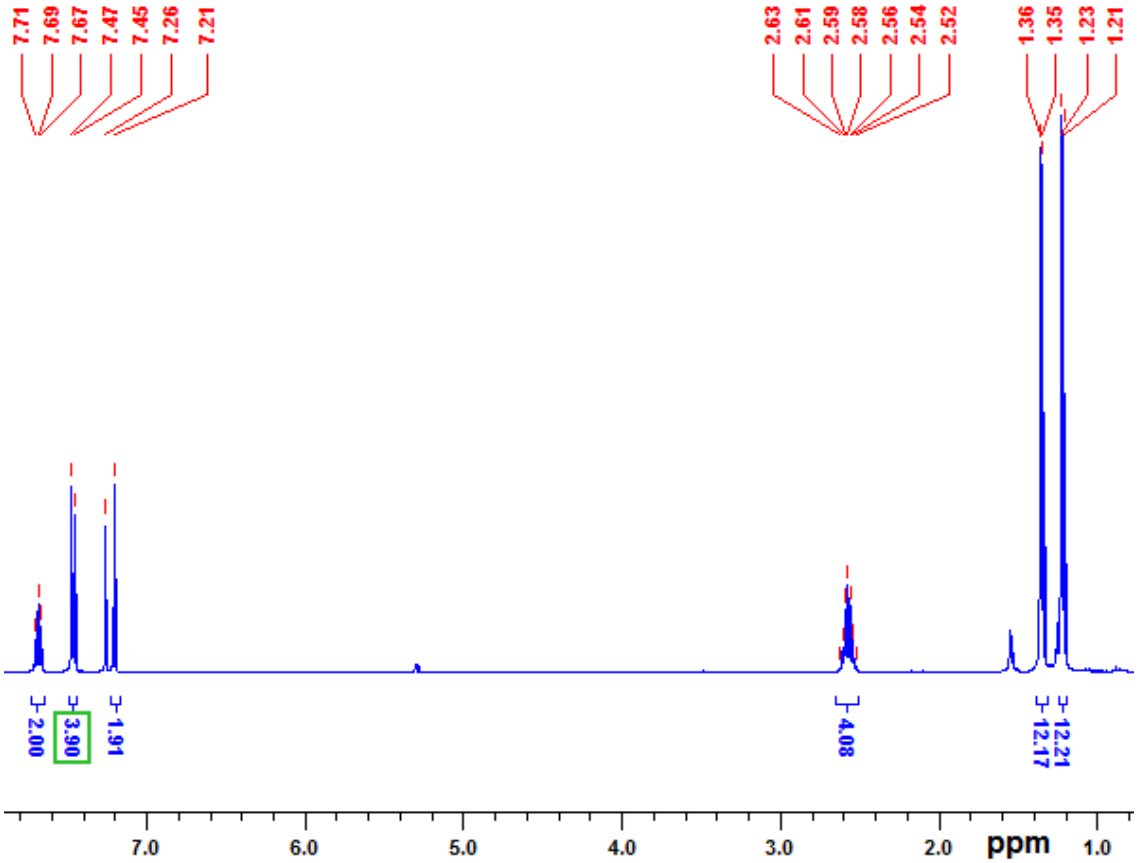

Figure S7. ^{1}H NMR spectrum of $[(IPr{=}S)BiCl_3].CHCl_3$ (**6**) in $CDCl_3$ at RT.

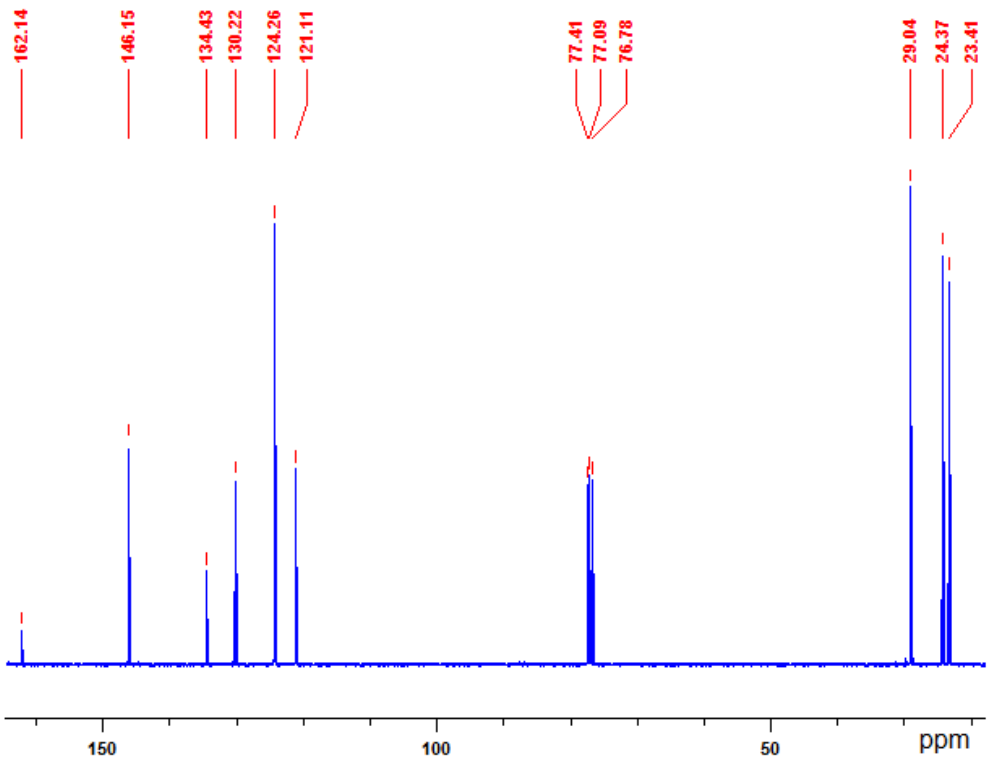

Figure S8. ^{13}C NMR spectrum of [(IPr=S)$BiCl_3$].$CHCl_3$ (**6**) in $CDCl_3$ at RT.

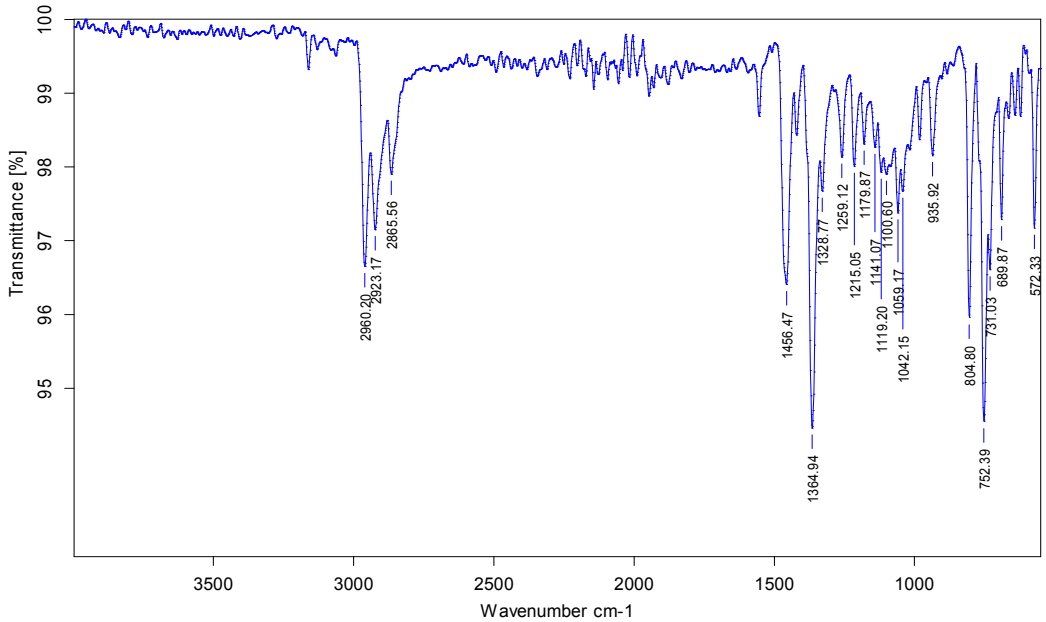

Figure S9. FT-IR (neat) spectrum of [(IPr=S)$BiBr_3$].$CHCl_3$ (**7**) at RT.

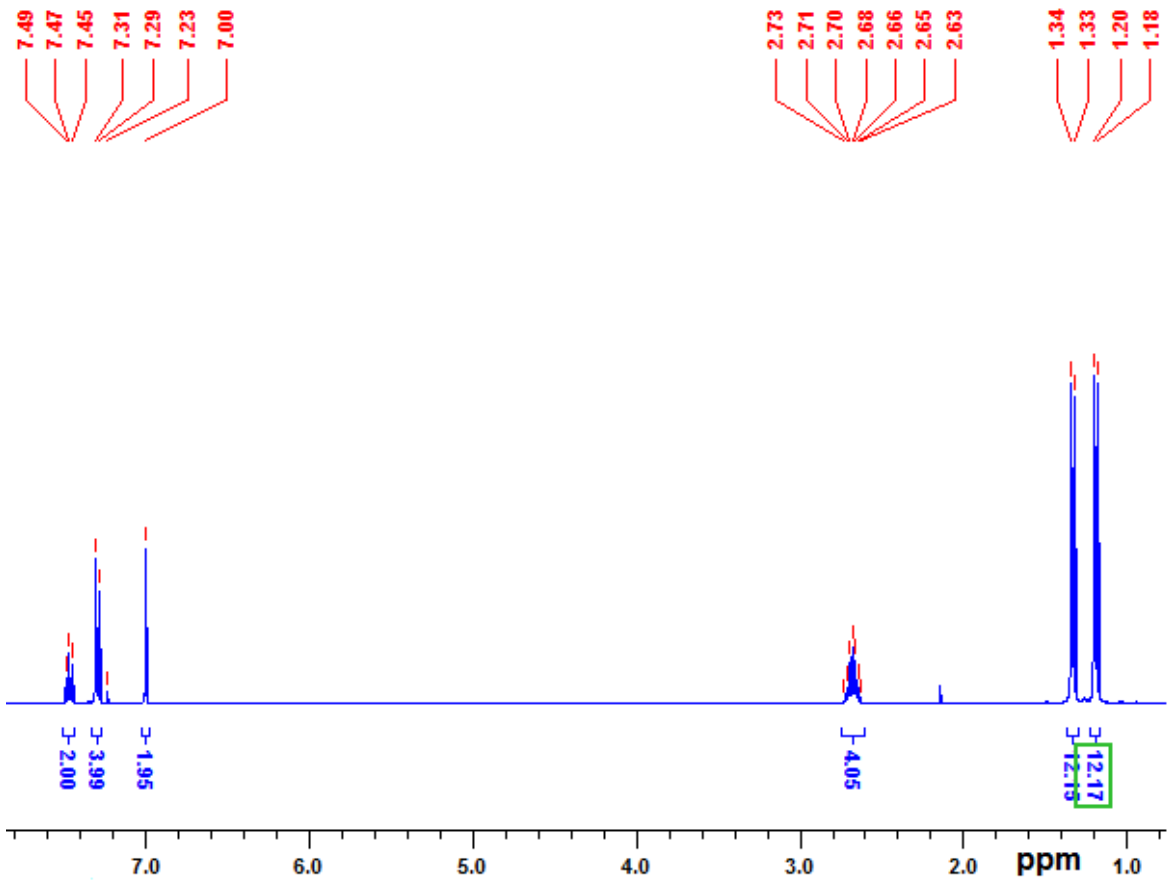

Figure S10. ^{1}H NMR spectrum of [(IPr=S)$BiBr_3$].$CHCl_3$ (**7**) in $CDCl_3$ at RT.

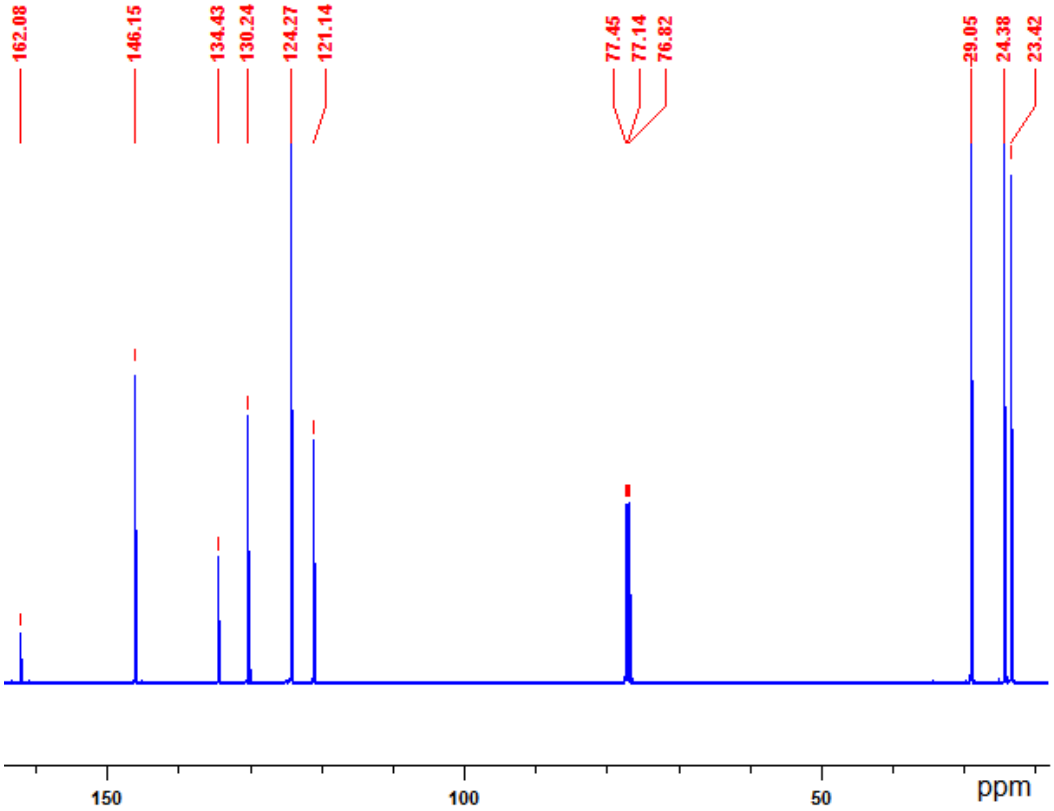

Figure S11. ^{13}C NMR spectrum of $[(IPr{=}S)BiBr_3].CHCl_3$ (**7**) in $CDCl_3$ at RT.

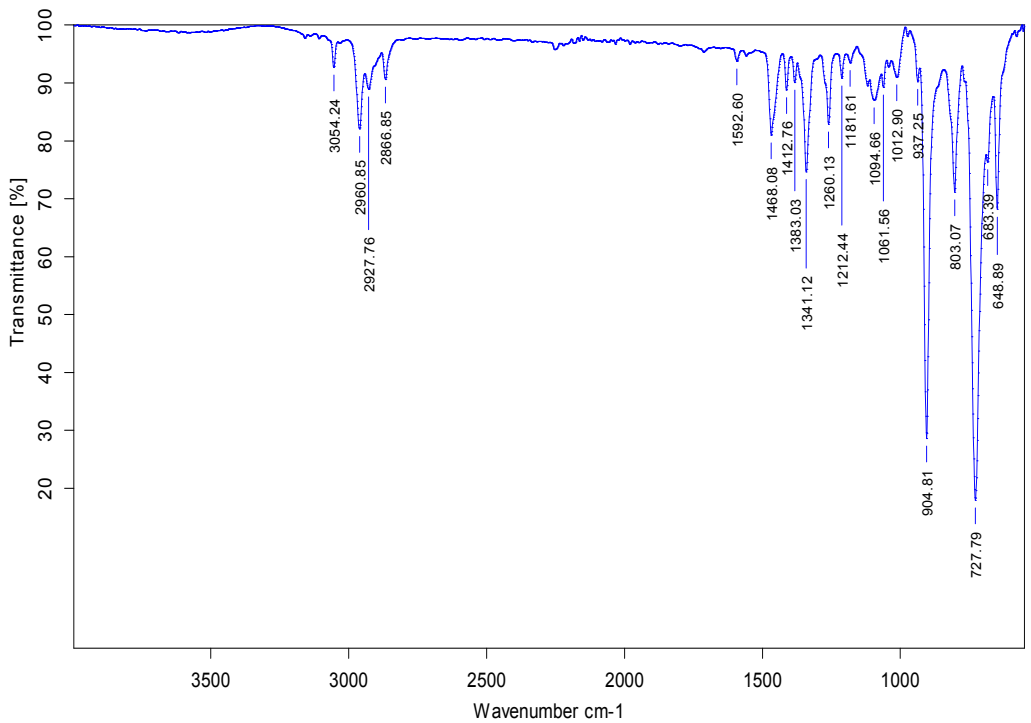

Figure S12. FT-IR (neat) spectrum of $[(IPr{=}Se)BiCl_3].CH_2Cl_2$ (**8**) at RT.

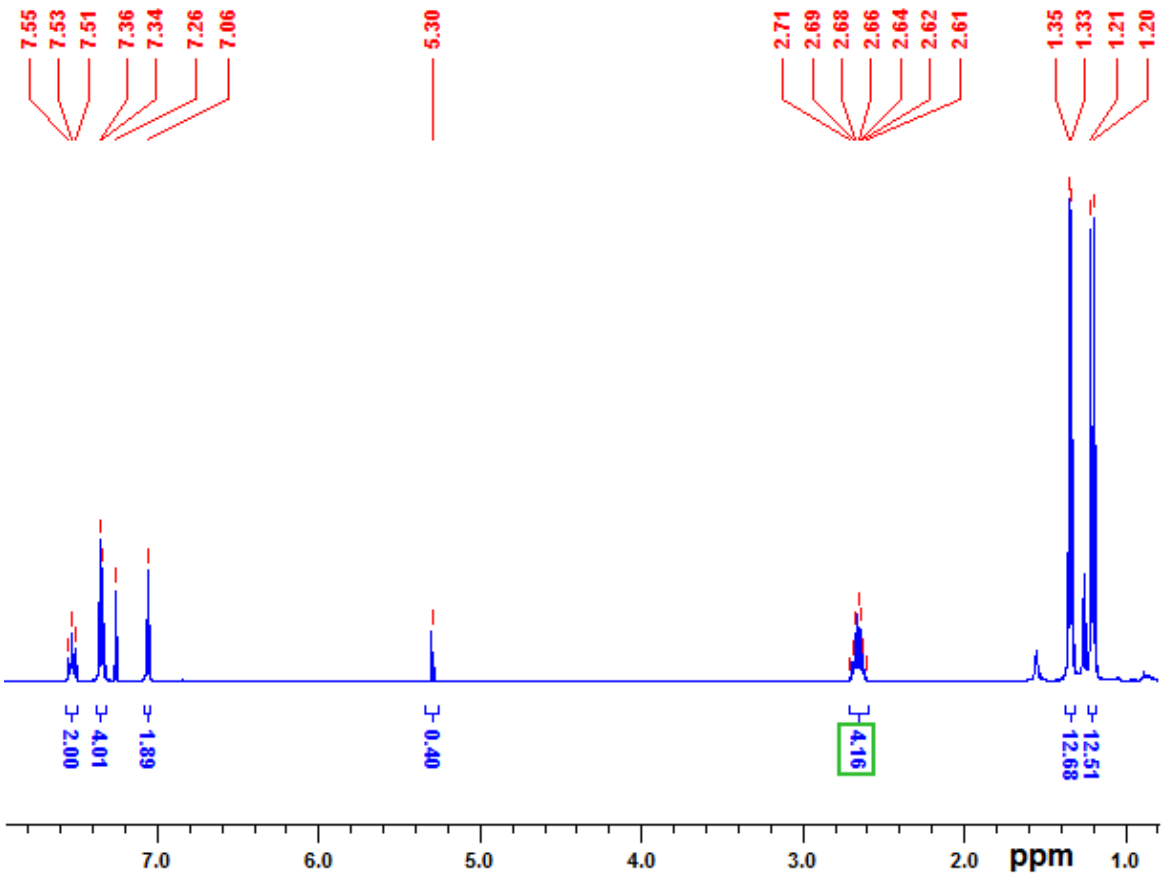

Figure S13. ^{1}H NMR spectrum of $[(IPr{=}Se)BiCl_3].CH_2Cl_2$ (**8**) in $CDCl_3$ at RT.

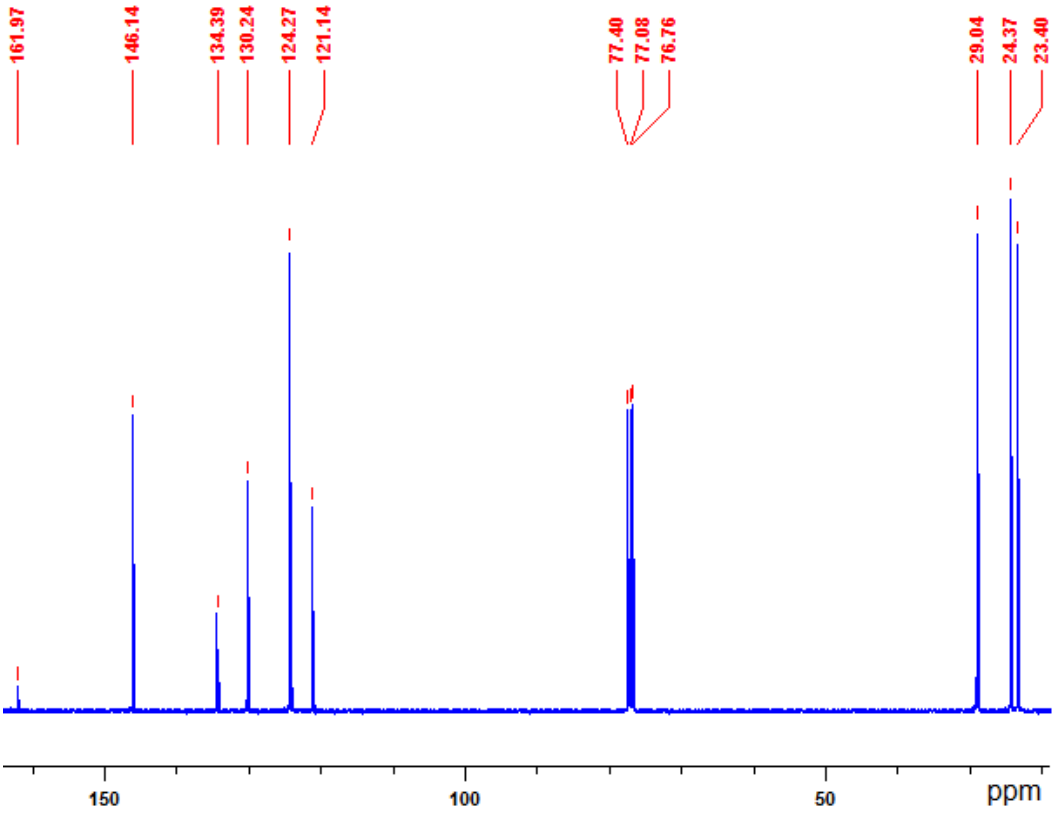

Figure S14. ^{13}C NMR spectrum of [(IPr=Se)$BiCl_3$].CH_2Cl_2 (**8**) in $CDCl_3$ at RT.

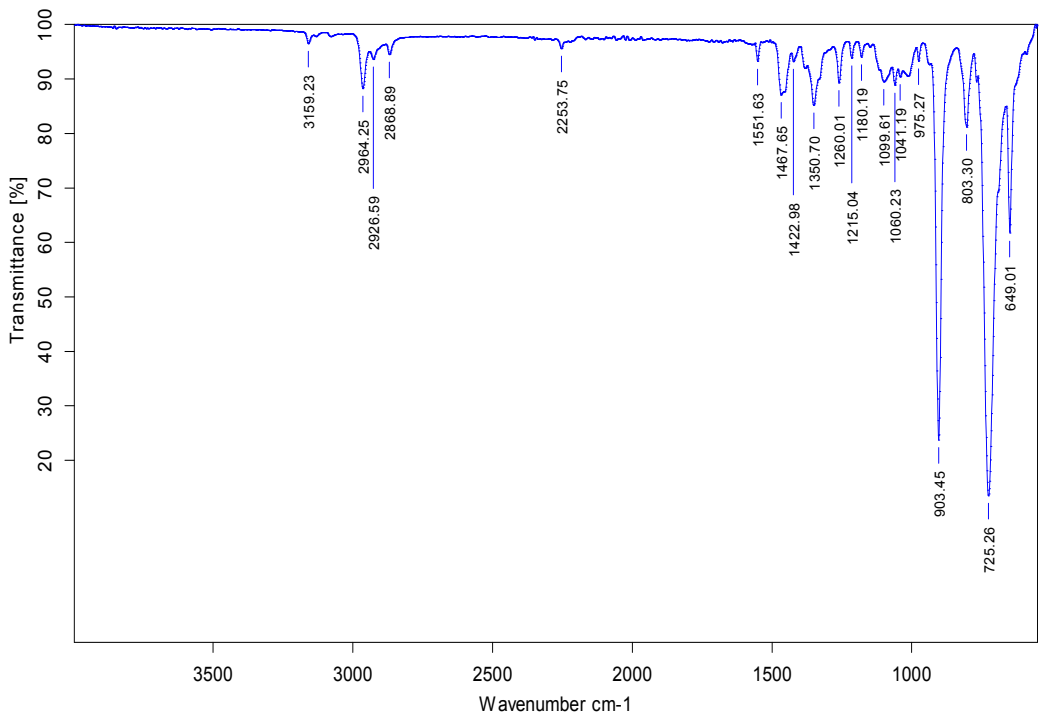

Figure S15. FT-IR (neat) spectrum of [(IPr=Se)$BiBr_3$].CH_2Cl_2 (**9**) at RT.

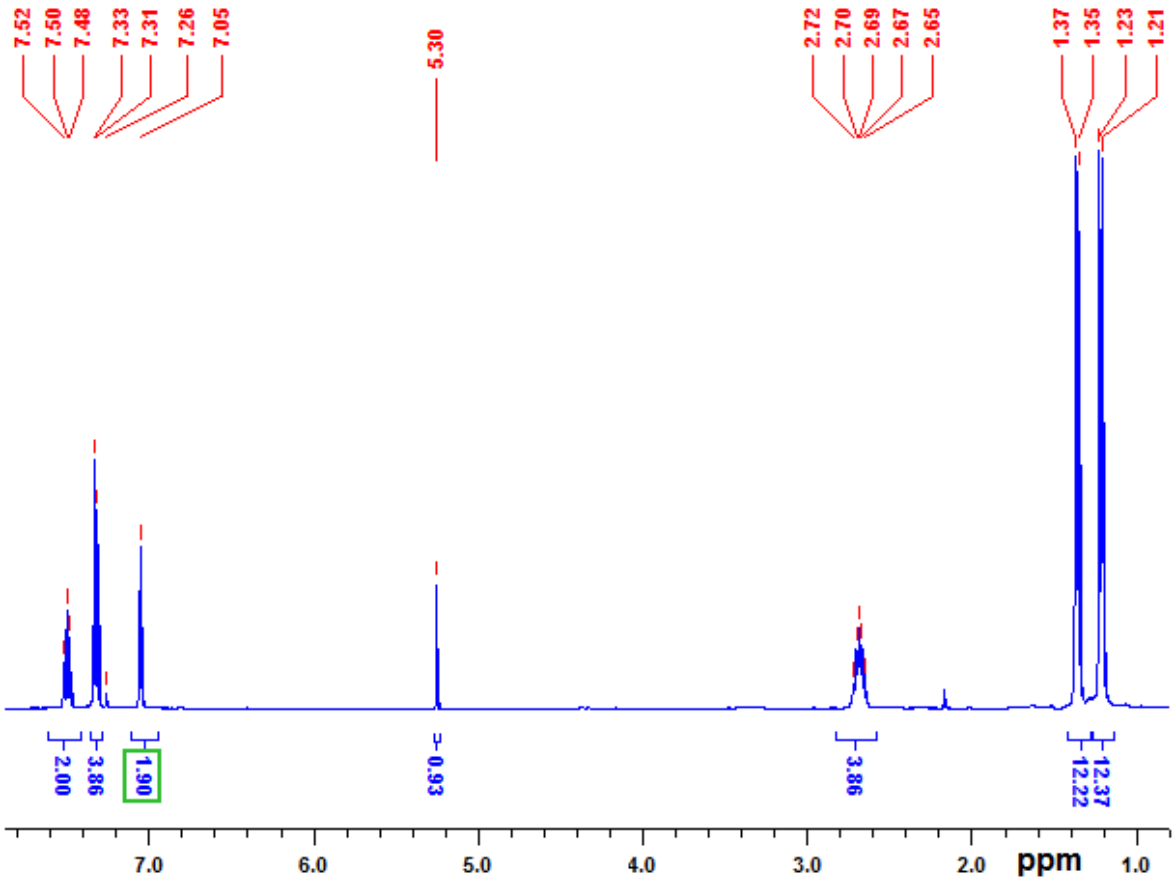

Figure S16. ^{1}H NMR spectrum of [(IPr=Se)$BiBr_3$].CH_2Cl_2 (**9**) in $CDCl_3$ at RT.

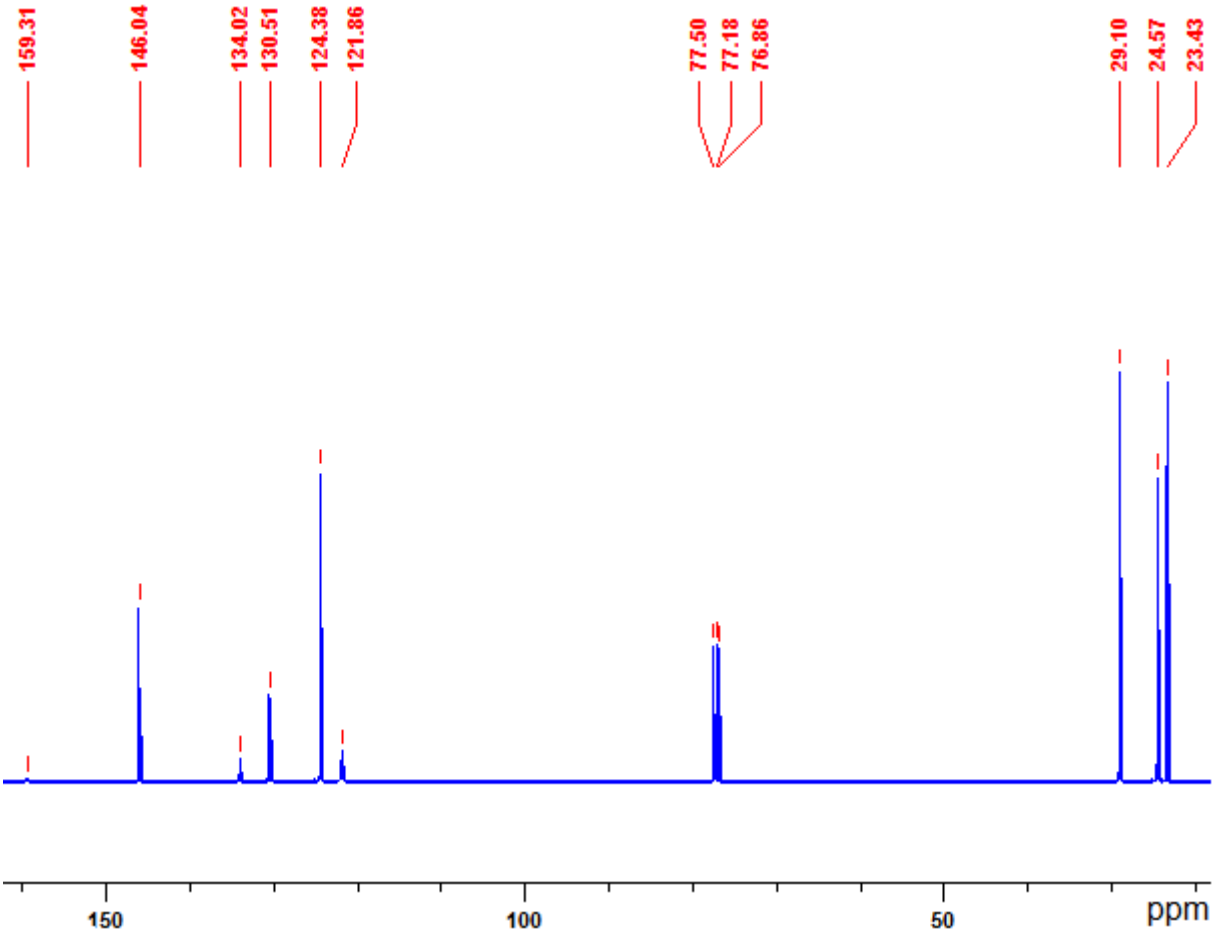

Figure S17. ^{13}C NMR spectrum of $[(IPr{=}Se)BiBr_3].CH_2Cl_2$ (**9**) in $CDCl_3$ at RT.

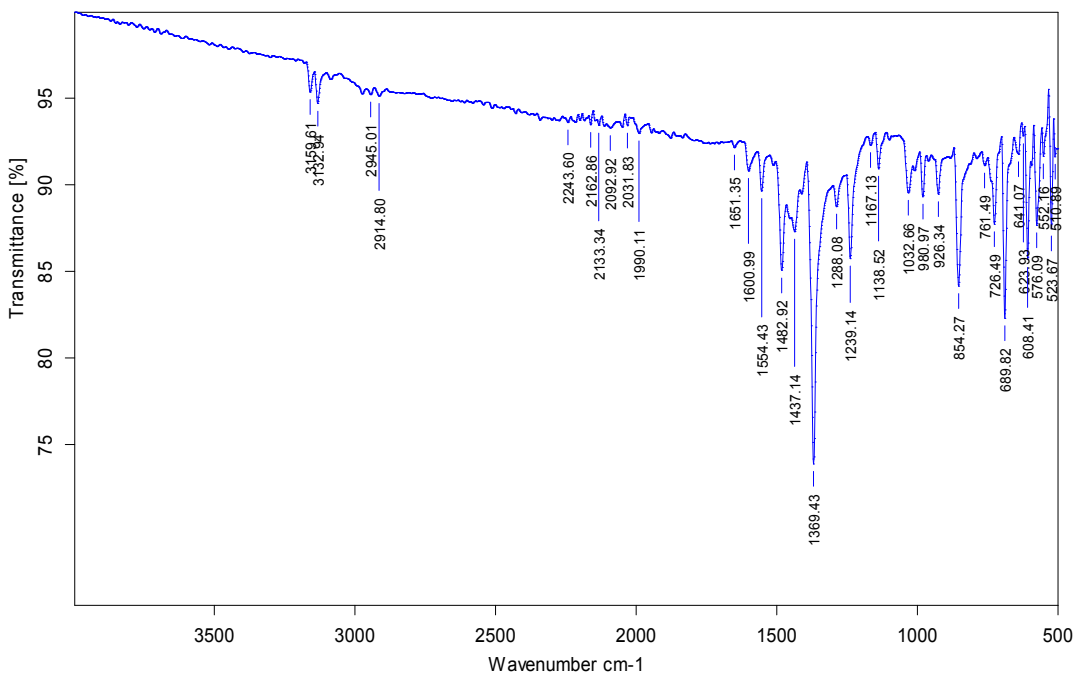

Figure S18. FT-IR (neat) spectrum of $[(IMesS)Bi(Cl)_2(\mu_2\text{-}Cl)]_2.4CHCl_3$ (**12**) at RT.

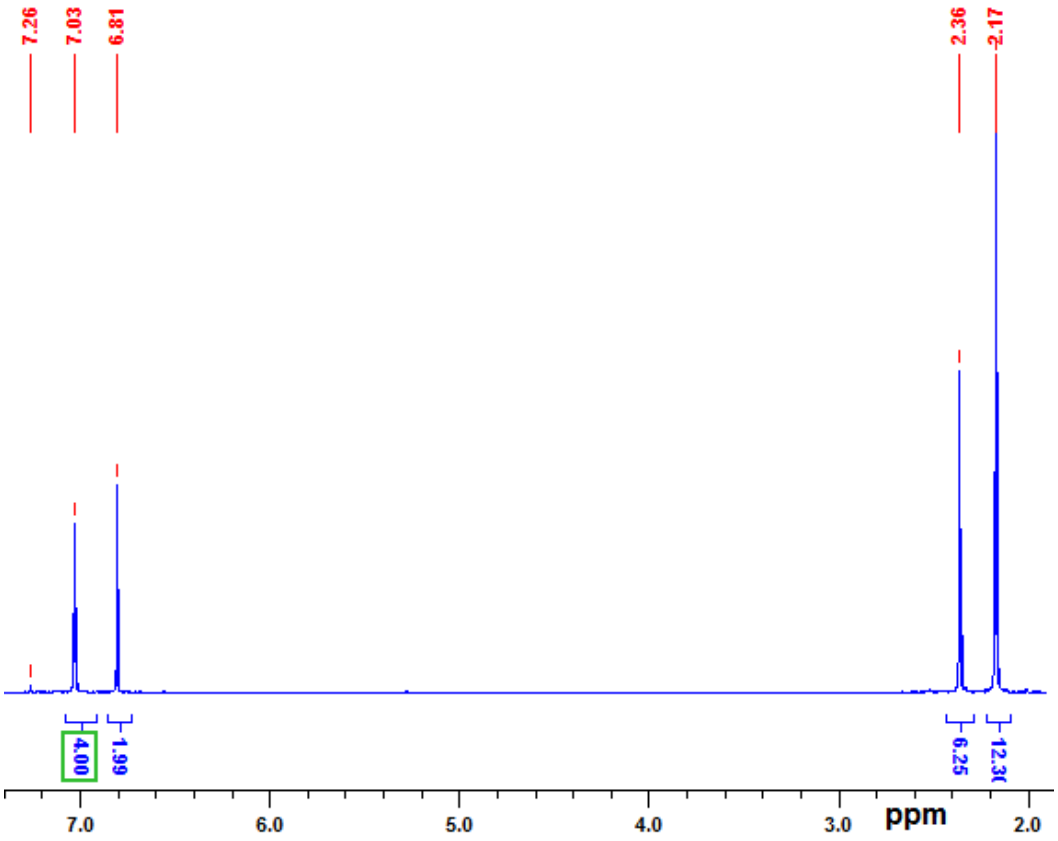

Figure S19. ^{1}H NMR spectrum of [(IMesS)Bi(Cl)$_2$(μ_2-Cl)]$_2$.4CHCl$_3$ (**12**) in CDCl$_3$ at RT.

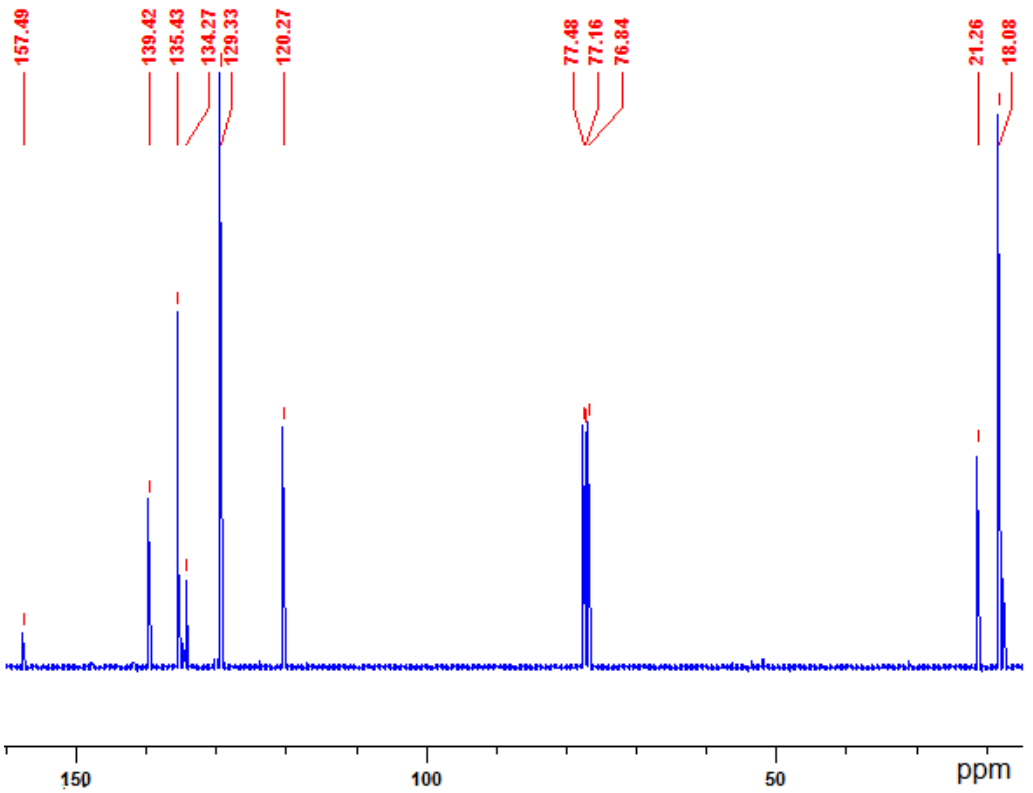

Figure S20. ^{13}C NMR spectrum of $[(IMesS)Bi(Cl)_2(\mu_2\text{-}Cl)]_2.4CHCl_3$ (**12**) in $CDCl_3$ at RT.

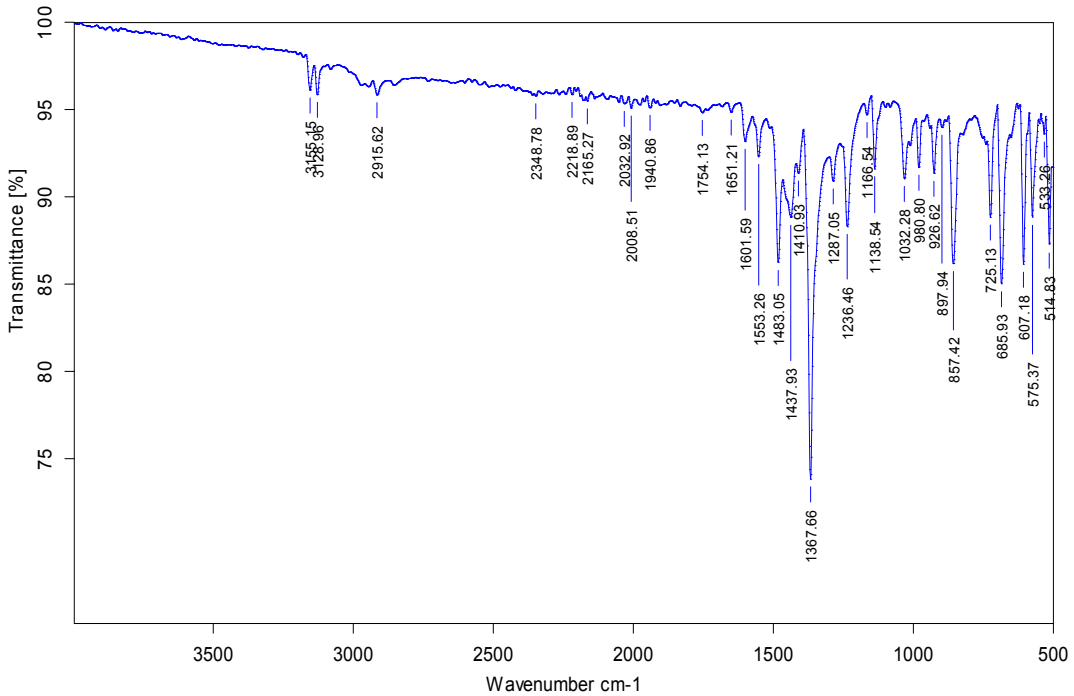

Figure S21. FT-IR (neat) spectrum of $[(IMesS)Bi(Br)_2(\mu_2\text{-}Br)]_2.2CHCl_3$ (**13**) at RT.

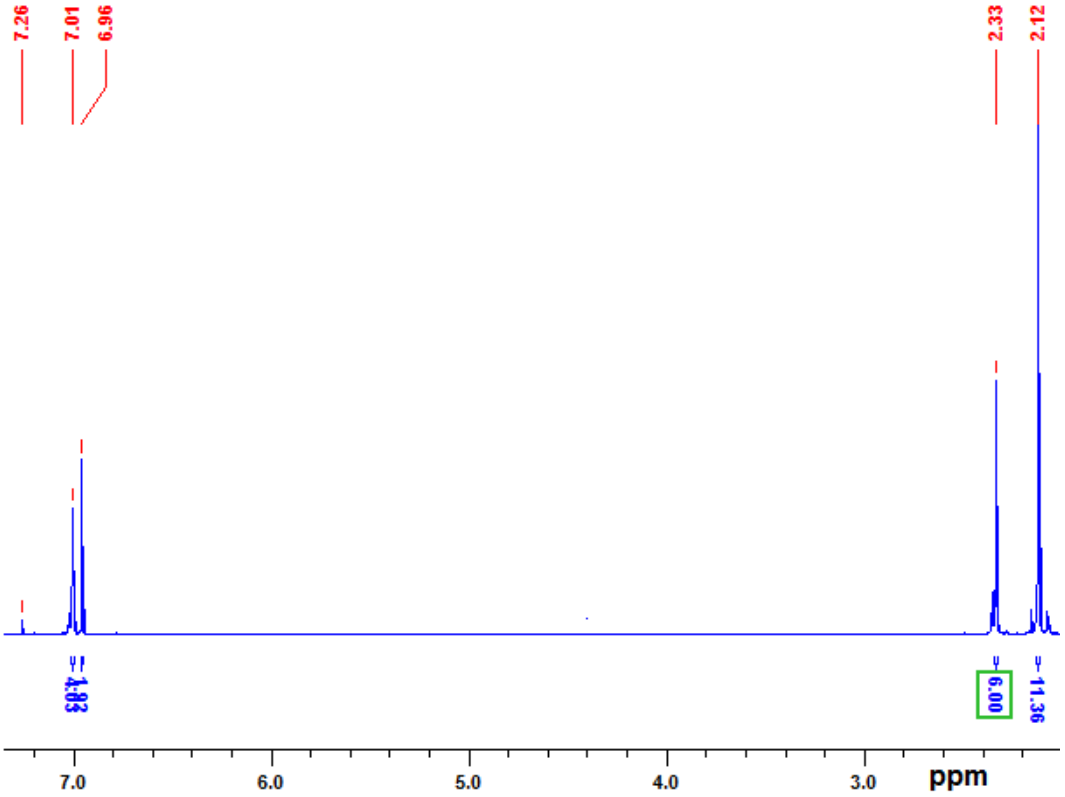

Figure S22. ^{1}H NMR spectrum of [(IMesS)Bi(Br)$_2$(μ_2-Br)]$_2$.2CHCl$_3$ (**13**) in CDCl$_3$ at RT.

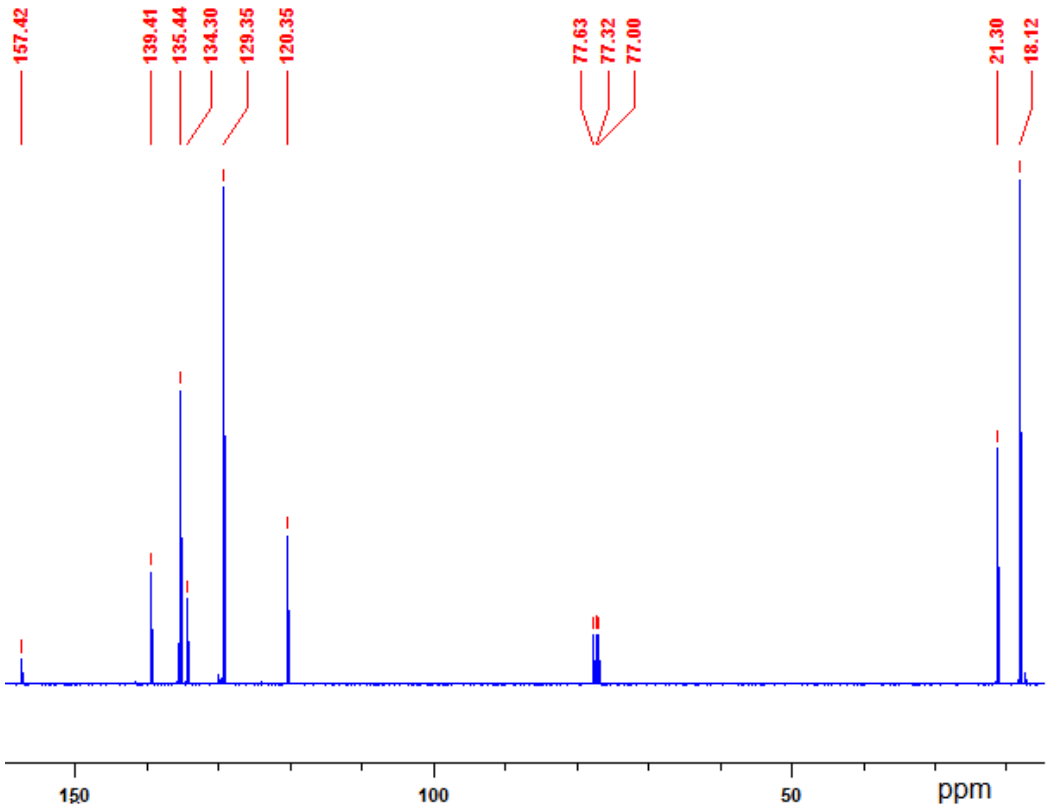

Figure S23. ^{13}C NMR spectrum of [(IMesS)Bi(Br)$_2$(μ_2-Br)]$_2$.2CHCl$_3$ (**13**) in CDCl$_3$ at RT.

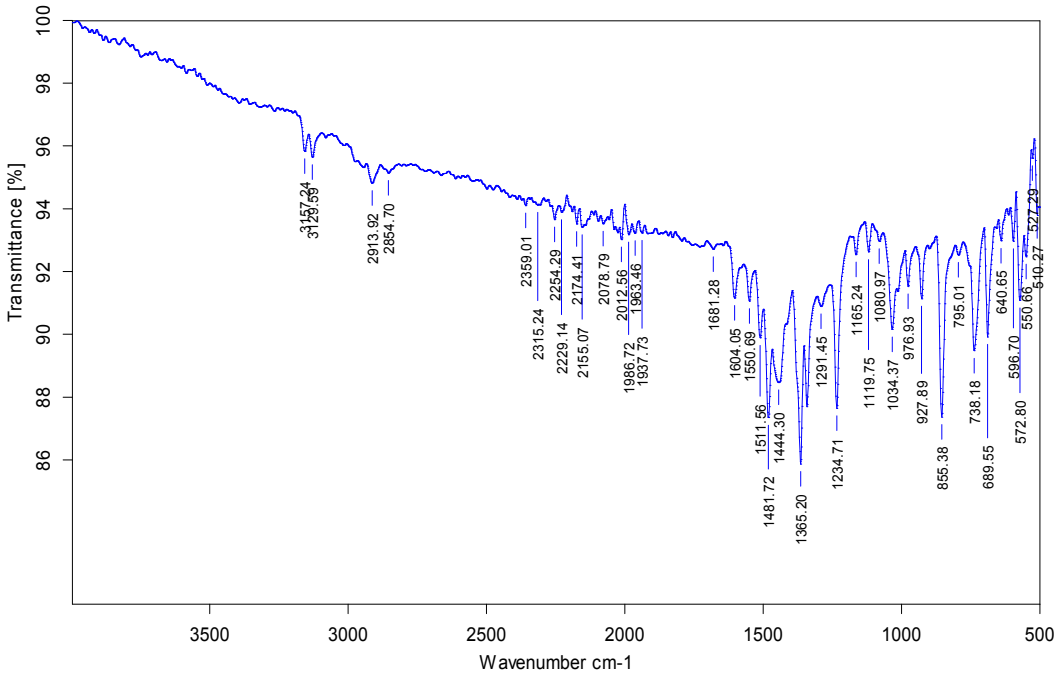

Figure S24. FT-IR (neat) spectrum of $[(IMesSe)Bi(Cl)_2(\mu_2\text{-}Cl)]_2.4CH_2Cl_2$ (**14**) at RT.

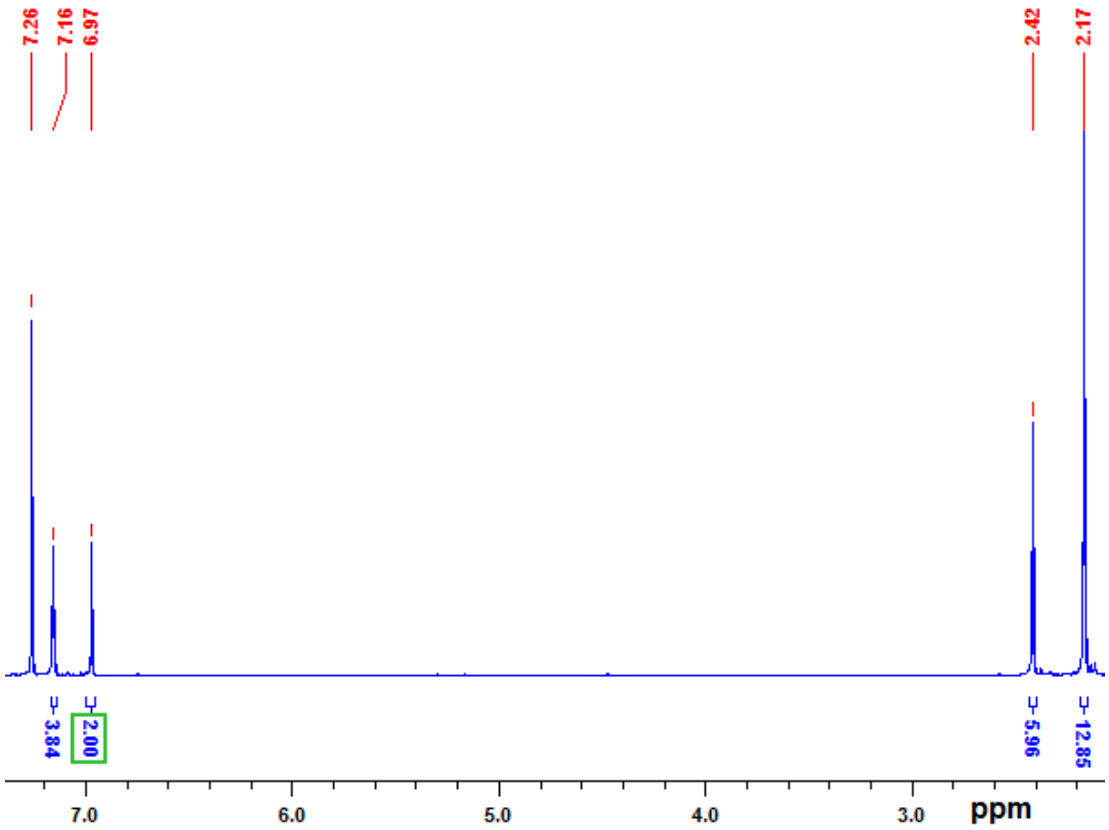

Figure S25. ^1H NMR spectrum of $[(IMesSe)Bi(Cl)_2(\mu_2\text{-}Cl)]_2.4CH_2Cl_2$ (**14**) in $CDCl_3$ at RT.

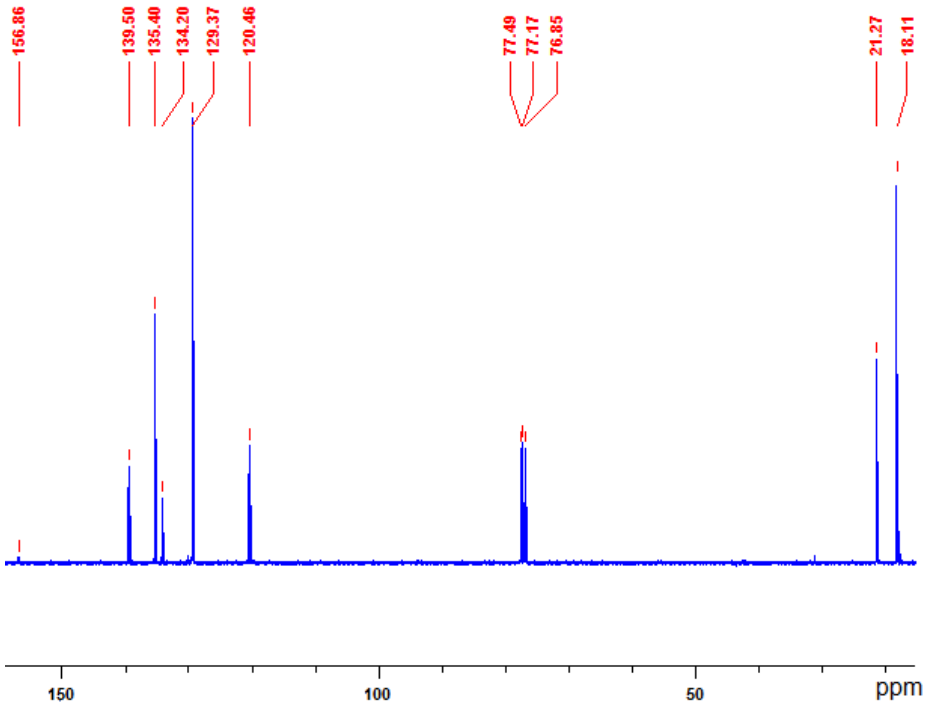

Figure S26. ^{13}C NMR spectrum of $[(IMesSe)Bi(Cl)_2(\mu_2\text{-}Cl)]_2.4CH_2Cl_2$ (**14**) in $CDCl_3$ at RT.

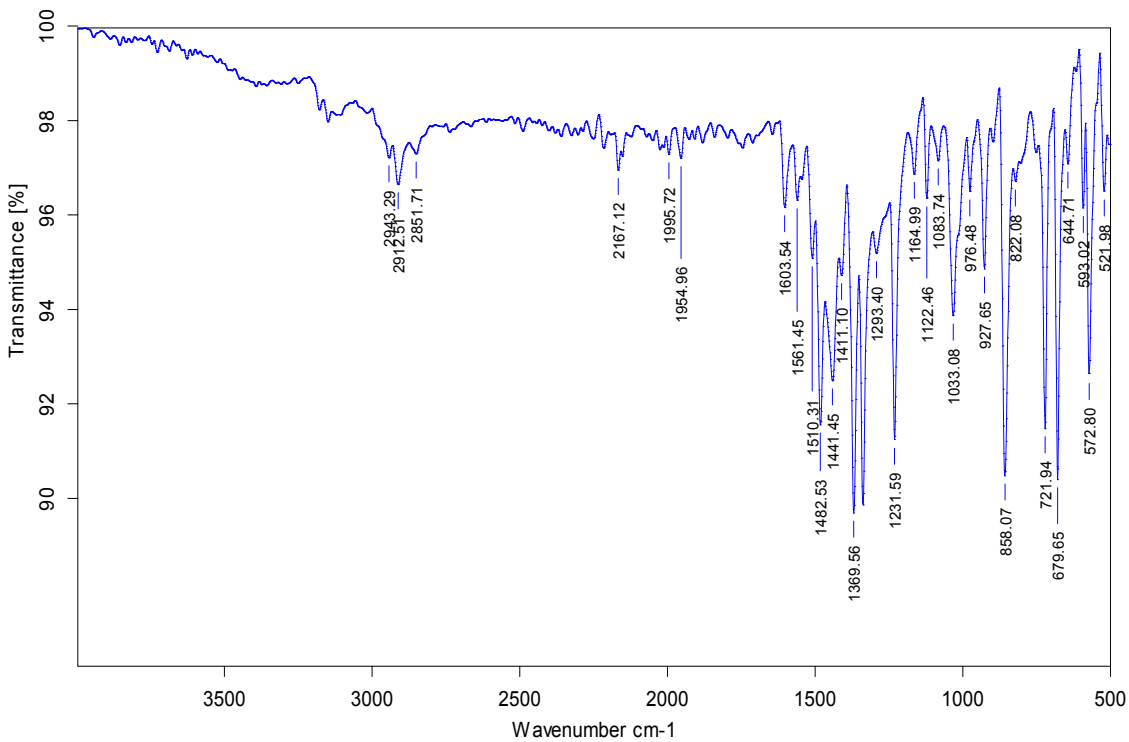

Figure S27. FT-IR (neat) spectrum of $[(IMesSe)Bi(Br)_2(\mu_2\text{-}Br)]_2$ (**15**) at RT.

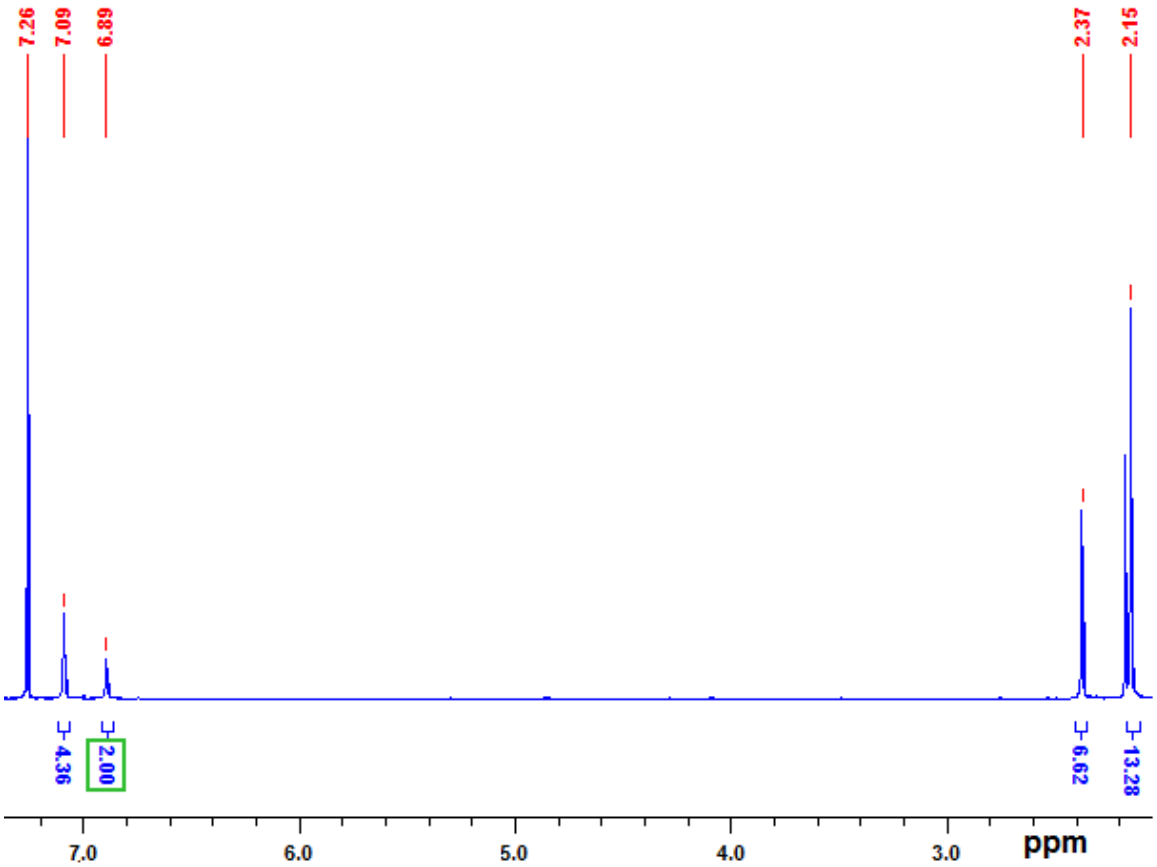

Figure S28. ^{1}H NMR spectrum of [(IMesSe)Bi(Br)$_2$(μ_2-Br)]$_2$ (**15**) in $CDCl_3$ at RT.

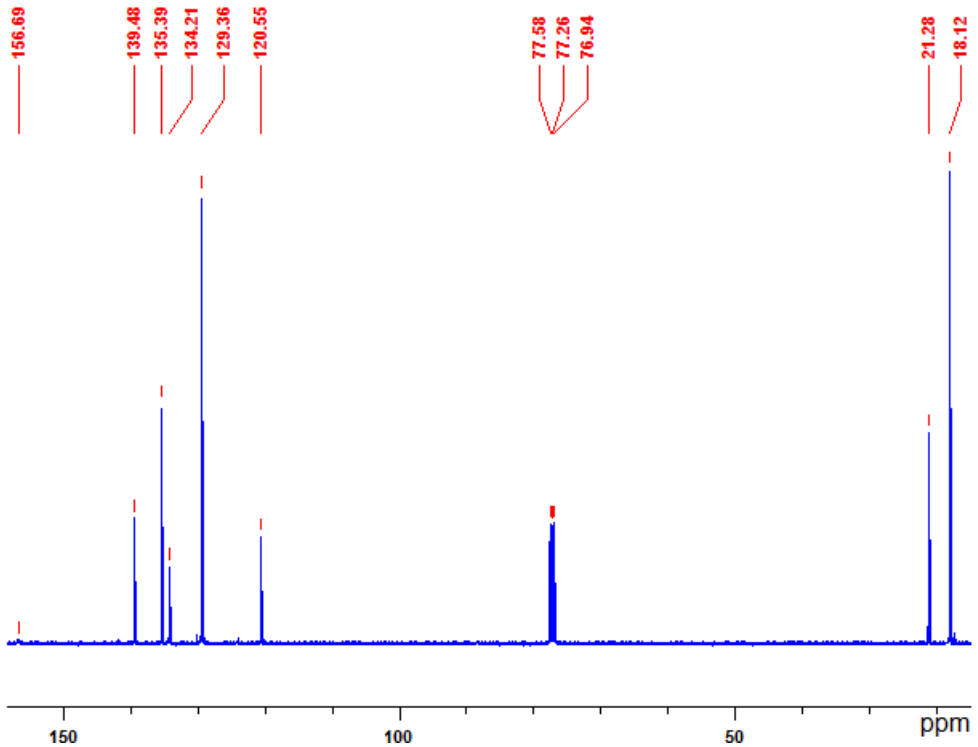

Figure S29. ^{13}C NMR spectrum of $[(IMesSe)Bi(Br)_2(\mu_2\text{-}Br)]_2$ (**15**) in $CDCl_3$ at RT.

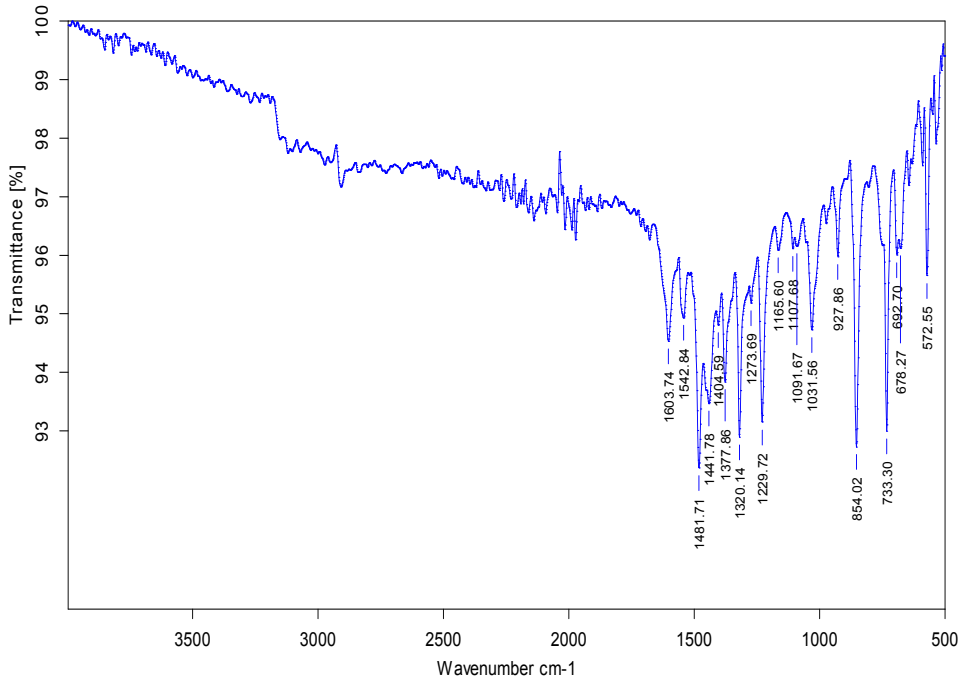

Figure S30. FT-IR (neat) spectrum of $[(IMesTe)Bi(Cl)_2(\mu_2\text{-}Cl)]_2$ (**16**) at RT.

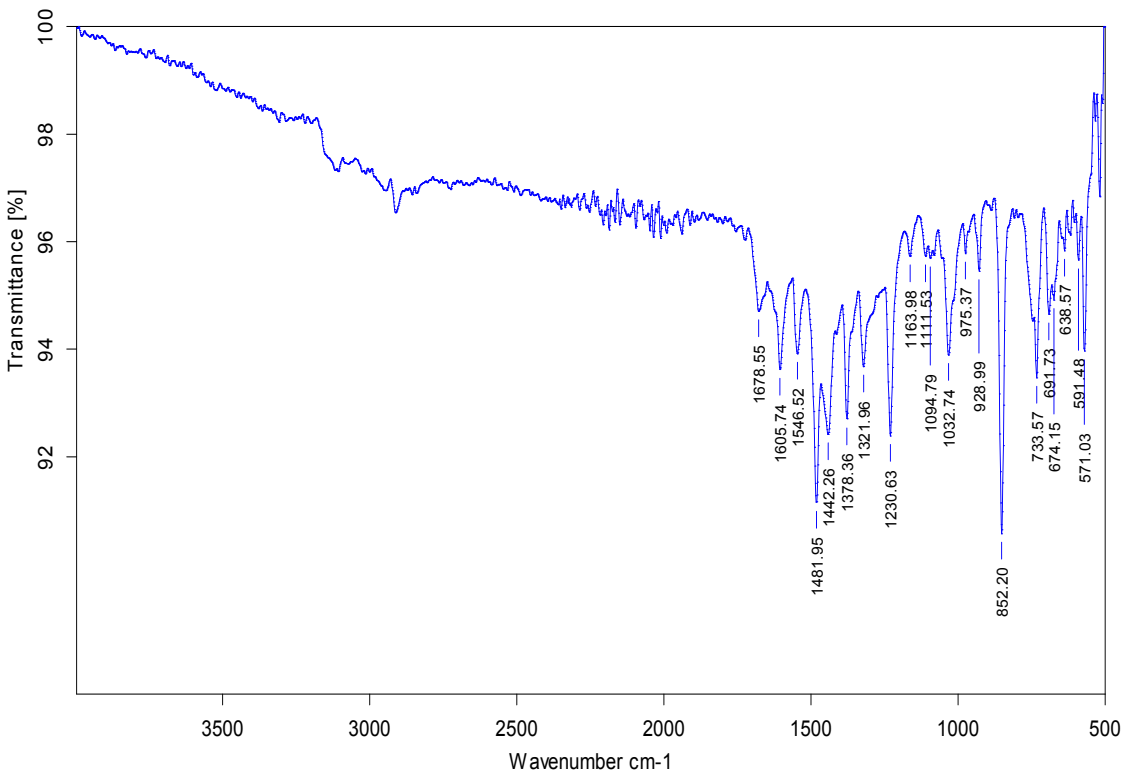

Figure S31. FT-IR (neat) spectrum of $[(IMesTe)Bi(Br)_2(\mu_2\text{-}Br)]_2$ (**17**) at RT.

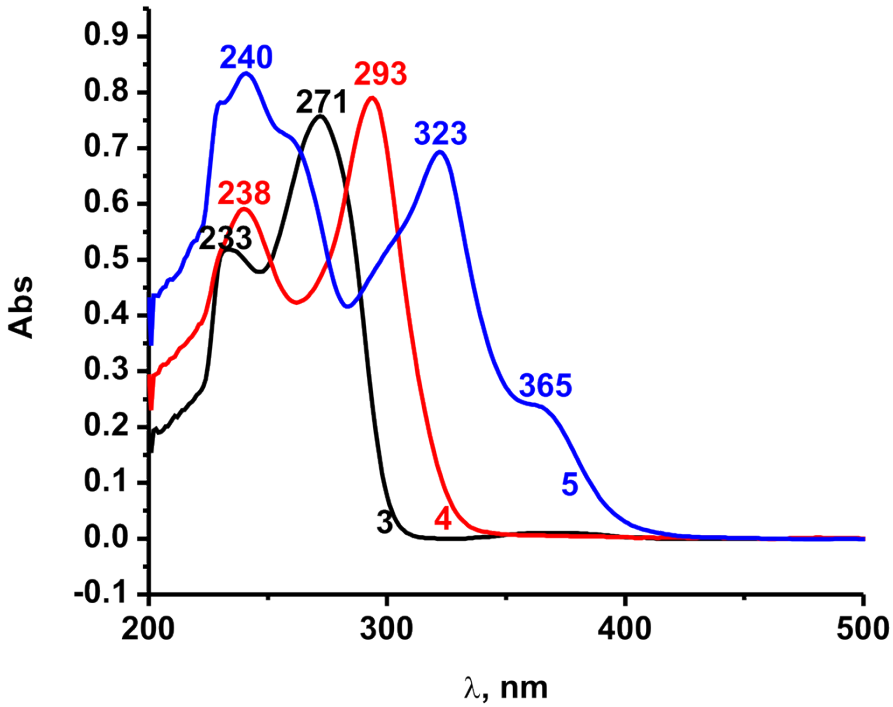

Figure S32. The solution state UV-vis spectra of **3-5** in DCM at 25°C (3.8 X 10^{-2} M).

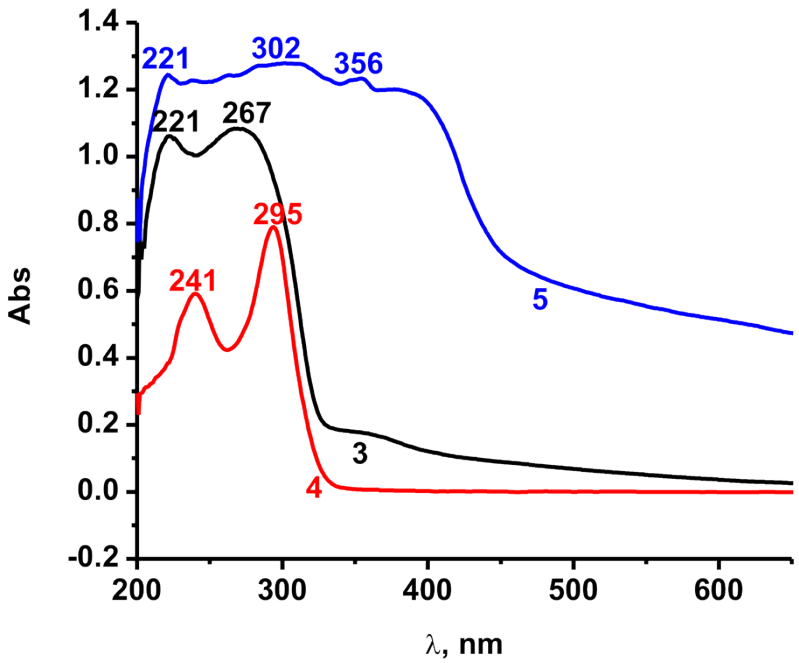

Figure S33. The solid state UV-vis spectra of **3-5.**

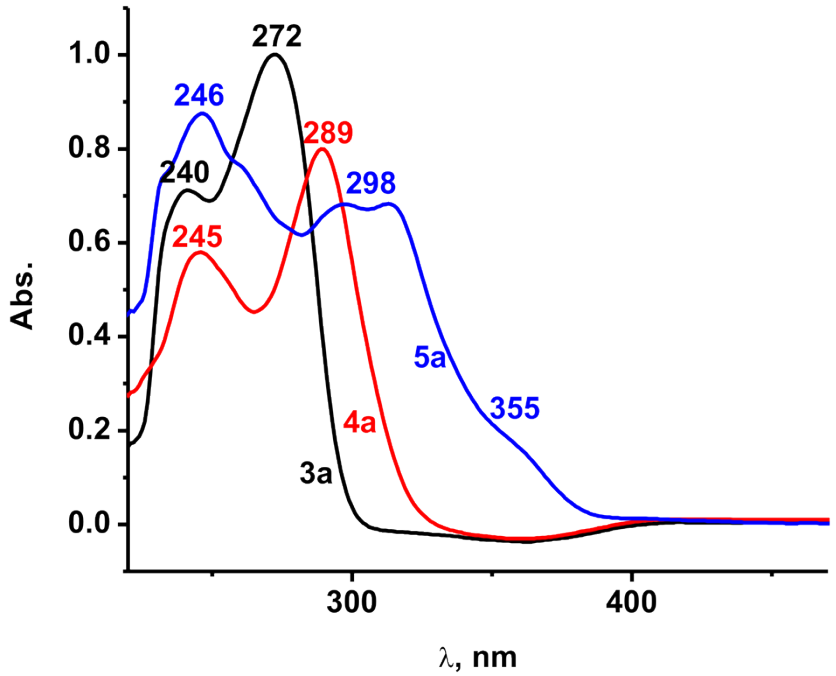

Figure S34. The solution state UV-vis spectra of **3a-5a** in DCM at 25°C (3.8 X 10^{-2} M).

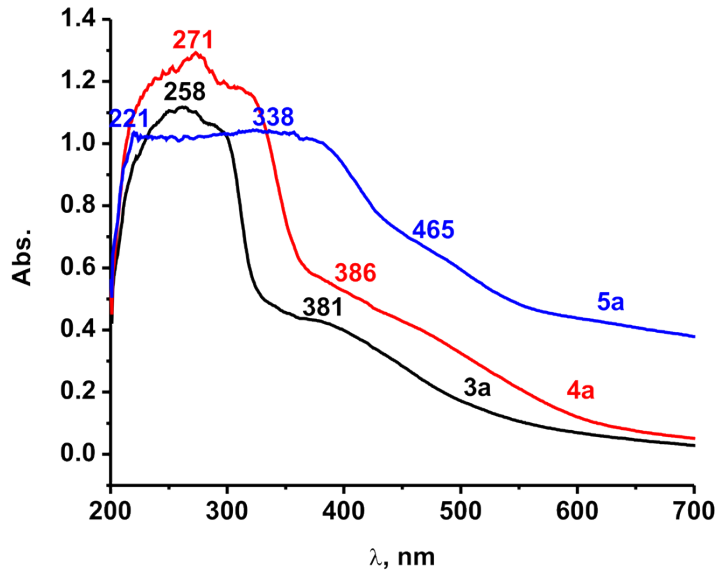

Figure S35. The solid state UV-vis spectra of **3a-5a.**

Table S1a. Structural parameters of compounds **3**, **5-9**.

	3	**5**	**6**	**7**	**8**	**9**
Empirical formula	$C_{6.75}H_9N_{0.5}S_{0.25}$	$C_{6.75}H_9N_{0.5}Te_{0.25}$	$C_7H_{9.25}N_{0.5}S_{0.25}Cl_{1.5}Bi_{0.25}$	$C_{14}H_{18.5}NS_{0.5}Br_{1.5}Bi_{0.5}Cl_{1.5}$	$C_7H_{9.5}N_{0.5}Cl_{1.25}Bi_{0.25}Se_{0.25}$	$C_{28}H_{38}BiBr_3Cl_2N_2Se$
Formula weight	420.67	516.20	855.38	988.73	867.83	1001.18
Temperature (K)	150	150	150	156	150	150
Crystal system	Monoclinic	Monoclinic	Monoclinic	Triclinic	Monoclinic	Monoclinic
Space group	$P2_1/n$	$P2_1/n$	$P2_1/c$	$P\bar{1}$	$P2_1/c$	$P2_1/c$
a/Å	19.2174(14)	19.1643(5)	9.6999(3)	10.0168(4)	10.75451(16)	10.7722(2)
b/Å	6.8155(4)	7.15496(17)	14.6885(5)	12.5839(6)	16.0772(2)	16.3835(3)
c/Å	20.0755(17)	20.1107(8)	23.7580(7)	15.6771(7)	19.7995(4)	20.0651(4)
α/°	90	90	90	73.883(4)	90	90
β/°	101.338(8)	106.852(4)	93.507(3)	76.522(4)	104.6833(16)	103.228(2)
γ/°	90	90	90	74.563(4)	90	90
Volume (Å^3)	2578.1(3)	2639.17(16)	3378.65(18)	1802.72(15)	3311.58(9)	3447.26(12)
Z	4	4	4	2	4	4
ρ_{calc}/mg mm^{-3}	1.0837	1.2991	1.6815	1.8214	1.7405	1.9289
Absorption coefficient (μ/mm^{-1})	1.205	8.989	15.342	16.228	15.567	16.890
F(000)	915.5	1058.3	1678.5	941.0	1680.5	1884.0
Reflections collected	9769	10829	13786	12304	15584	14315
R_{int}	0.0313	0.0333	0.0566	0.0507	0.0364	0.0399
GOF on F^2	1.064	1.040	1.023	1.029	1.041	1.033
R_1 ($I>2\sigma(I)$)	0.0626	0.0354	0.0727	0.0593	0.0384	0.0550
wR_2 ($I>2\sigma(I)$)	0.178639	0.095047	0.242118	0.163590	0.106819	0.156333
R_1 values (all data)	0.0832	0.0444	0.0828	0.0605	0.0417	0.0593
R_2 values (all data)	0.1786	0.0950	0.2421	0.1636	0.1068	0.1563

Table S1b. Structural parameters of compounds **4a** and **12-15**.

	4a	**12**	**13**	**14**	**15**
Empirical formula	$C_{21}H_{24}N_2Se$	$C_{46}H_{52}Bi_2Cl_{18}N_4S_2$	$C_{46}H_{52}Bi_2Br_6Cl_{12}N_4S_2$	$C_{23}H_{28}BiCl_7N_2Se$	$C_{42}H_{48}N_4Se_2Bi_2Br_6$
Formula weight	383.40	1781.19	2047.90	1737.20	1664.18
Temperature (K)	150	150	150	150	150
Crystal system	Orthorhombic	Monoclinic	Triclinic	Monoclinic	Monoclinic
Space group	*Pbcn*	$P2_1/n$	$P\bar{1}$	$P2_1/c$	$P2_1/c$
a/Å	16.0321(9)	12.2653(8)	9.9610(5)	15.9721(6)	9.5278(2)
b/Å	7.3653(3)	17.1990(9)	13.3493(6)	10.8271(4)	16.1998(4)
c/Å	16.0280(5)	15.5570(7)	14.3207(7)	18.3916(6)	16.2869(4)
α/°	90	90	111.257(5)	90	90.00
β/°	90	99.117(5)	103.339(4)	97.510(3)	98.199(2)
γ/°	90	90	97.547(4)	90	90.00
Volume (Å^3)	1892.61(14)	3240.3(3)	1677.59(16)	3153.19(19)	2488.15(10)
Z	4	2	1	2	2
ρ_{calc}/mg mm^{-3}	1.3455	1.8255	2.0971	1.8296	2.221
Absorption coefficient (μ/mm^{-1})	2.695	18.252	19.615	17.875	21.293
F(000)	790.6	1722.9	963.2	1659.3	1544.0
Reflections collected	3592	12843	11831	14171	10803
R_{int}	0.0281	0.0569	0.0684	0.0374	0.0392
GOF on F^2	1.210	1.046	1.050	1.041	1.048
R_1 ($I>2\sigma(I)$)	0.0426	0.1190	0.0604	0.0531	0.0358
wR_2 ($I>2\sigma(I)$)		0.321768	0.166247	0.161189	0.0951
R_1 values (all data)	0.0529	0.1368	0.0614	0.0635	0.0406
R_2 values (all data)	0.1721	0.3218	0.1662	0.1612	0.1005

Table S2. Selected bond lengths and angles of compounds **6-9**.

	6	**7**	**8**	**9**
Bond lengths [Å]				
Bi(1)–E(1)	2.929(2)	2.940(18)	2.971(5)	2.980(8)
Bi(1)–X(1)	2.578(3)	2.615(8)	2.473(12)	2.620(9)
Bi(1)–X(2)	2.452(3)	2.731(9)	2.486(13)	2.760(9)
Bi(1)–X(3)	2.479(2)	2.610(8)	2.594(13)	2.630(10)
C(1)–E(1)	1.696(10)	1.694(7)	1.861(5)	1.861(8)
Bond angles [°]				
N(1)–C(1)–N(2)	106.1(8)	105.9(6)	106.1(4)	105.9(6)
N(1)–C(1)–E(1)	130.1(7)	125.5(5)	125.3(3)	129.2(5)
N(2)–C(1)–E(1)	123.7(7)	128.7(5)	108.5(3)	124.8(5)
C(1)–E(1)–Bi(1)	108.8(3)	114.1(2)	110.94(13)	111.5(2)
X(1)–Bi(1)–X(2)	93.08(9)	93.28(3)	90.93(5)	91.21(3)
X(1)–Bi(1)–X(3)	90.27(10)	94.71(3)	89.40(5)	92.86(3)
X(2)–Bi(1)–X(3)	94.70(9)	93.76(3)	94.48(5)	94.19(3)
X(1)–Bi(1)–E(1)	70.47(9)	80.75(4)	75.33(3)	76.53(3)
X(2)–Bi(1)–E(1)	84.60(8)	172.70(5)	103.09(3)	160.92(3)
X(3)–Bi(1)–E(1)	80.73(8)	90.94(5)	156.73(4)	100.88(3)

Table S3. Selected bond lengths and angles of compounds **4a**, **12-15**.

	4a	**12**	**13**	**14**	**15**
Bond lengths [Å]					
Bi(1)–E(1)		2.874(5)	2.778(2)	2.8931(10)	2.9251(7)
Bi(1)–X(1)		2.509(4)	2.6827(9)	2.523(2)	2.7084(8)
Bi(1)–X(2^1)		2.693(5)	2.9146(9)	2.763(2)	3.0744(7)
Bi(1)–X(3)		2.482(5)	2.6330(9)	2.485(2)	2.6152(7)
C(1)–E(1)	1.827(6)	1.683(19)	1.703(9)	1.870(9)	1.866(6)
Bond angles [^{o}]					
N(1)–C(1)–N(1)	104.8(5)	104.1(15)	109.9(7)	106.3(7)	105.9(5)
N(1)–C(1)–E(1)	127.6(3)	131.3(12)	123.1(6)	129.0(7)	129.6(4)
N(2)–C(1)–E(1)		124.6(14)	130.2(6)	124.7(7)	124.5(4)
X(1)–Bi(1)–X(2^1)		88.08(15)	90.64(3)	87.88(8)	169.94(2)
X(1)–Bi(1)–E(1)		94.60(15)	93.55(5)	91.26(6)	97.88(2)
X(3)–Bi(1)–X(1)		90.73(15)	90.08(3)	90.45(8)	88.10(3)
X(3)–Bi(1)–X(2^1)		90.66(19)	93.52(3)	87.82(7)	87.30(2)
X(3)–Bi(1)–E(1)		77.37(15)	81.18(5)	75.14(5)	79.27(2)
E(1)–Bi(1)–X(2^1)		167.75(17)	173.24(5)	162.94(5)	90.05(2)
C(1)–E(1)–Bi(1)		112.6(6)	110.8(3)	109.8(3)	108.54(19)

Table S4. Preparation of 4-chloropentylacetate.

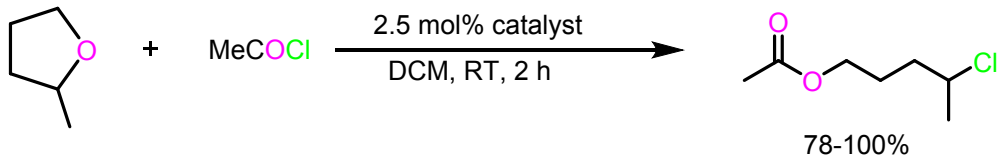

78-100%

Entry	Catalyst	Starting Material Conversion (%)[a]	Yield (%)[b]
1	IPrS-$BiBr_3$ (**7**)	88	80
2	IPrSe-$BiCl_3$ (**8**)	96	90
3	IPrSe-$BiBr_3$ (**9**)	85	78
4	IPrTe-$BiCl_3$ (**10**)	80	76
5	IPrTe-$BiBr_3$ (**11**)	78	75
6	IMesS-$BiCl_3$ (**12**)	94	90
7	IMesS-$BiBr_3$ (**13**)	88	80
8	IMesSe-$BiCl_3$ (**14**)	92	88
9	IMesSe-$BiBr_3$ (**15**)	86	82
10	IMesTe-$BiCl_3$ (**16**)	84	80
11	IMesTe-$BiBr_3$ (**17**)	79	70
12	IPrS & $BiCl_3$	95	90
13	$BiCl_3$	92	88
14	$BiBr_3$	90	85
15	Without catalyst	0	0

[a] The starting materials conversion was calculated after 2h.

[b] % Yields were calculated based on the weight of products and the starting material conversion.

Table S5. Bismuth(III) mediated *O*-acylative cleavage of different cyclic ethers.

Entry	Starting Materials		Product	Time (h)[a]	Starting Material Conversion (%)	Yield (%)[c]
1		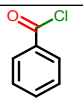	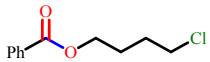	48	94	88
2	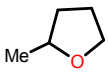		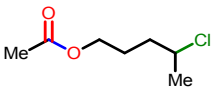	2	100	99
3	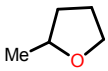	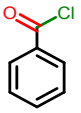	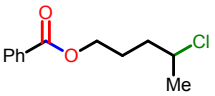	4	100	99
4			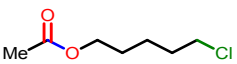	48	30	28
5		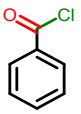	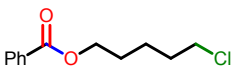	48	20	18
6			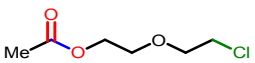	48	15[b]	12
7		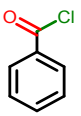	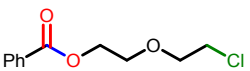	48	10[b]	8

a = The obtimized time is 2h, however the reaction time was increased since the reaction was too slow. b =No further conversion after 48 h; c = % Yields were calculated based on the weight of the product with respect to the starting material.